Quantum Electronics **49** (6) 600–603 (2019)

FREQUENCY STANDARDS

https://doi.org/10.1070/QEL16889

Multifrequency source for pumping CPT-resonances based on an external cavity diode laser

A.A. Isakova, N.N. Golovin, K.N. Savinov, A.K. Dmitriev

Abstract. **We report the results of studying operation regimes for an external-cavity diode laser in which the intermode interval corresponds to the clock transition frequency under modulation of the injection current by an rf oscillator, which provides multifrequency pumping of CPT-resonances.**

Keywords: *coherent population trapping, CPT-resonance, diode laser, rf pumping.*

1. Introduction

An interference of two ground states with one common level that is excited by two coherent radiations at the frequencies coinciding with two allowed optical transitions yields a dip in an observed fluorescence spectrum when the difference of light wave frequencies equals to the clock transition frequency. This phenomenon predicted in [1] and first observed in a cell with sodium atoms [2] was called coherent population trapping (CPT).

One of the main applications of CPT-resonances is their employment as a frequency reference in frequency standards [3]. Presently, the most abundant are rubidium clocks, first samples of which were optically pumped by a spectral lamp with rubidium vapours [4].

Now, rubidium clocks are often pumped by vertical cavity diode lasers which have the advantages of low energy consumption and compact size [5, 6]. The emission spectrum of such a laser can be efficiently modulated in a wide range of microwave frequencies including the clock transition frequency F_0. In addition, efficient microwave pumping of a diode laser having the intermode interval equal to half the clock transition frequency $F_0/2$ has been demonstrated [7].

A single-laser optical pumping of CPT-resonances in rubidium atoms was realised under sinusoidal modulation of the injection current of an AlGaAs diode laser operated at an emission wavelength of 780 nm [8]. Under the sub-harmonic modulation at the frequency $F_0/6 = 1.139$ GHz with a modulation index of 4.2, a resonance with a relative width of 4.4×10^{-7} was detected. Note that in the latter case only two spectral components optically pumped a CPT-resonance, which were separated by a frequency F_0. The hyperfine transition of the ground state $5S_{1/2}(F = 2)-5S_{1/2}(F = 1)$ of the D_1-line of the ^{87}Rb isotope at a wavelength of 795 nm has smaller shifts and provides approximately ten times higher intensity of CPT-resonances as compared to the case of the D_2-line (780 nm), which is related to a difference in the magnetic sublevel structure of the excited P-state [9].

One of the main factors reducing stability of rubidium frequency standards is the light shift, whose value is proportional to a product of the difference of saturation parameters of the pump frequencies and their shifts relative to the frequencies of optical transitions. For reducing this shift it was suggested to use a wide emission spectrum of a femtosecond laser, in which the pulse repetition rate is related to the clock transition frequency [10]. However, since only the frequencies fitting the spectrum of optical transitions contribute into the CPT-resonance formation, the signal-to-noise ratio will be extremely low while observing the resonance under pumping by a femtosecond laser.

Active mode locking of a diode laser with the pump current modulated at a frequency of 260 MHz, which matches the laser cavity intermode interval made it possible to obtain a multifrequency emission in the near-threshold regime [11]. Nevertheless, the width of the emission spectrum obtained is substantially less than the clock transition frequency, and large laser dimensions determined by the cavity length also limit possible applications of the method.

In the present work we present the results of studying operation regimes of an external cavity diode laser in which the intermode interval corresponds to the clock transition frequency, under modulation of the laser injection current by an rf oscillator. This provides multifrequency pumping of CPT-resonances.

2. Multifrequency emission for detecting CPT-resonances

Without pump current modulation by an rf oscillator, the diode laser operates at one of the cavity modes. Under frequency modulation, the spectrum of possible laser emission frequencies is described by a Bessel function. At high indices of frequency modulation $\varepsilon = \Delta f/f$ when the frequency deviation Δf is much greater than the modulation frequency f and is on the order of the laser intermode frequency $c/2L$ (c is the speed of light and L is the laser cavity length), the spectral components arise whose frequencies fit neighbouring laser cavity modes with an interval equal to f. An example in Fig. 1 presents cavity modes of a diode laser in which the intermode

A.A. Isakova, N.N. Golovin, K.N. Savinov Novosibirsk State Technical University, prosp. Karla Marksa 20, 630073 Novosibirsk, Russia; e-mail: alina100@mail.ru;
A.K. Dmitriev Novosibirsk State Technical University, prosp. Karla Marksa 20, 630073 Novosibirsk, Russia; Institute of Laser Physics, Siberian Branch, Russian Academy of Sciences, prosp. Akad. Lavrent'eva 13/3, 630090 Novosibirsk, Russia

Received 30 October 2018; revision received 20 December 2018
Kvantovaya Elektronika **49** (6) 600–603 (2019)
Translated by N.A. Raspopov

interval is half the clock transition frequency and $\varepsilon = 40$. For the maximum of the Bessel function to coincide with the side modes of the laser cavity, the modulation frequency f should approximately equal the ratio $\Delta f/\varepsilon$, which entails that f is ~ 85 MHz; it is substantially less than the width of the upper level of allowed optical transitions, which in view of buffer gas action is conventionally ~ 1 GHz. In the latter case, more than ten pairs of optical frequencies may realise optical pumping of CPT-resonances, which provides resonance summation, increases the signal, and reduces the light shift [10].

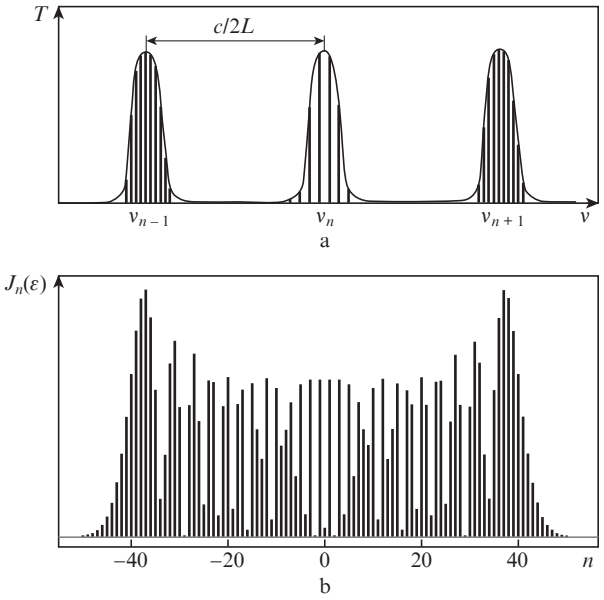

Figure 1. (a) Laser cavity modes filled with rf components at the deviation $\Delta f = 3.4$ GHz, and (b) the absolute value of the Bessel function for the modulation index $\varepsilon = 40$.

If the width of the cavity transmission band $\Delta\nu$ is substantially greater than the modulation frequency f, then lasing may occur at several spectral rf components (Fig. 1a).

Similarly to the employment of femtosecond radiation [10], extrema of CPT-resonances should occur at the modulation frequencies

$$f_k = F_0/k, \tag{1}$$

where k is an integer. From this follows that at the modulation frequency f, the structure of resonances will be observed with the interval reducing as k increases:

$$f_{k-1} - f_k = F_0 \frac{1}{(k-1)k}. \tag{2}$$

Here, the necessary condition for observing resonances is the presence of the spectral components of laser radiation, which coincide with the frequencies of allowed optical transitions.

For realising efficient modulation it is necessary to match the optical length of a laser cavity, L, with the clock transition frequency [7]:

$$F_0 = q\frac{c}{2L}, \tag{3}$$

where q is an integer that may have various values (in our case $q = 2$).

3. Experimental setup

An optical scheme of the diode laser was thoroughly described in [7]. One of the laser diode faces had an antireflection coating; the diode radiation passed to an aspheric lens and then onto a diffraction grating (1800 lines mm^{-1}). The cavity length was taken so that the intermode interval was about half the frequency of the clock transition $5S_{1/2}(F = 2)$–$5S_{1/2}(F = 1)$ of the ^{87}Rb isotope D_1-line, which is 6.8 GHz.

A scheme for measuring laser emission spectra is presented in Fig. 2. Signals from a dc current power supply (*1*) and from an SG384-SRS rf oscillator (*3*) passed through a ZFBT-6GW-FT mixer (*2*) to a diode laser (*4*). The load resistance (a laser diode) was ~ 1 Ω, which is substantially less than the internal resistance (50 Ω). This provided direct power–current conversion of the rf oscillator. The laser radiation passed through an optical insulator (*5*) to an optical spectrometer – a scanning Fabry–Perot interferometer (FPI) (*6*), formed by plane mirrors with transmissions 5% and 40% for the input and output mirrors, respectively. The output FPI mirror was attached to a piezoceramic transducer (*9*), which was used for scanning the spectrometer frequency by a digital sawtooth voltage source (*10*). The input mirror of the FPI was attached to another piezoceramic transducer (*7*) and moved by a dc voltage source (*6*). This provided detection of a spectral dependence $T(\nu)$ in the middle of the saw-signal slope, which reduced an influence of piezoceramic nonlinearity on the accuracy of the measured spectroscopic data. After the interferometer, radiation passed to a photodetector (*11*), the signal from which was recorded by a digital oscilloscope (*12*); a signal from the sawtooth voltage source passed to a second entry of the oscilloscope.

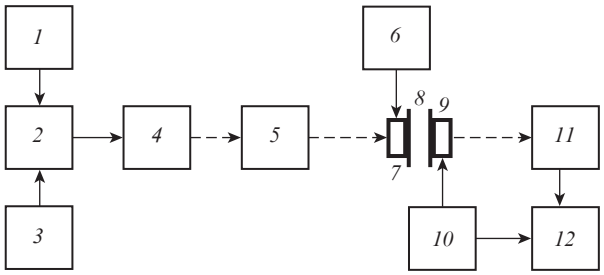

Figure 2. Scheme for measuring the laser emission spectrum: (*1*) laser power supply; (*2*) mixer; (*3*) rf oscillator; (*4*) diode laser; (*5*) optical insulator; (*6*) dc voltage source; (*7*, *9*) piezoceramic transducers; (*8*) Fabry–Perot interferometer; (*10*) sawtooth voltage generator; (*11*) photodetector; (*12*) digital oscilloscope.

4. Experimental results and discussion

The measurements were taken at a wavelength of 795 nm at a laser pump current of 53 mA and rf oscillator power of up to 10 dB. The laser threshold injection current was 49 mA.

Without modulation, the laser operated in a single-frequency regime. The free spectral range of the scanning FPI was about 25 GHz, and measured FWHM of its transmission was ~2 GHz. For reducing measurement errors, both the frequency (15 Hz) and voltage (240 V) of the sawtooth signal source used for tuning the FPI frequency were maintained constant.

Spectra were recorded at modulation frequencies of 68, 85, and 100 MHz, which satisfy condition (1). Laser emission spectra at $f = 85$ MHz and at various current amplitudes of rf modulation are shown in Fig. 3. All spectra bands are enumerated; the zero band corresponds to the carrier without rf modulation, the high-frequency side bands (1, 2) are marked with '+', the low-frequency bands (1, 2, 3) are marked with '–'. At a higher rf modulation power, the 'centre-of-mass' of the laser emission spectrum shifts to the high-frequency side. The frequency interval between neighbouring bands of the spectrum is close to the intermode interval. At other modulation frequencies and the corresponding rf-oscillator power, the spectral bands separated by $\sim c/2L$ were also observed.

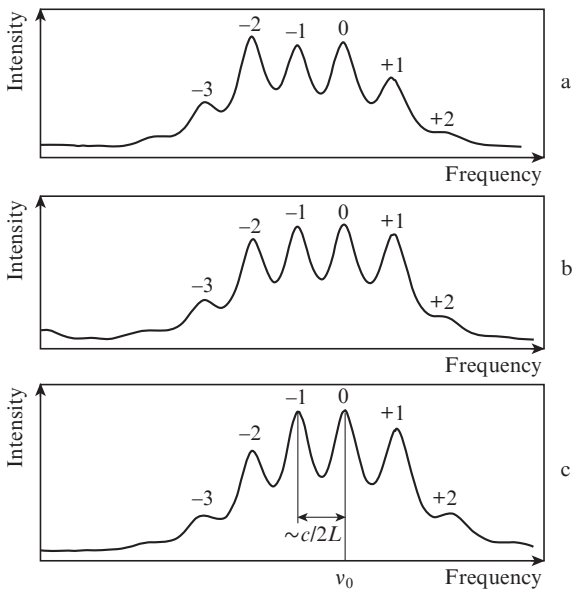

Figure 3. Laser emission spectra at the RF modulation current amplitudes (85 MHz) I_{RF} = (a) 7, (b) 8.4 and (c) 9.9 mA.

Dependences of spectral band amplitudes on the rf-oscillator current are shown in Fig. 4. The amplitudes are normalised to the intensity of laser emission without modulation. The measurement error was determined by photodetector noise and was ~2%. Actually, over the whole range of rf currents, the amplitude of the zero band is greater than of the rest bands. We relate the nonmonoton variation of spectral band amplitudes to an oscillating dependence of Bessel function components on the modulation index and to additional influence of amplitude modulation. In this case the character of the dependence of the sum of band amplitudes will be the same (Fig. 5).

Under rf modulation, the laser emission power weakly varies until $I_{RF} = 4$ mA, which is the excess of the injection current over a threshold value. Then the laser emission power increases linearly with the rf current (see Fig. 5). One can see

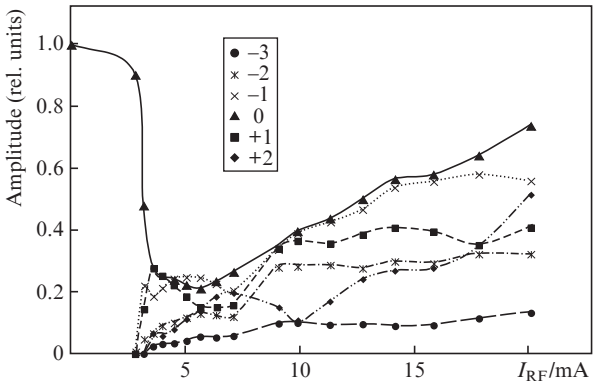

Figure 4. Dependences of the amplitudes of the laser emission spectrum envelope on the amplitude of the rf-oscillator current I_{RF}. Curves are enumerated according to notations in Fig. 3.

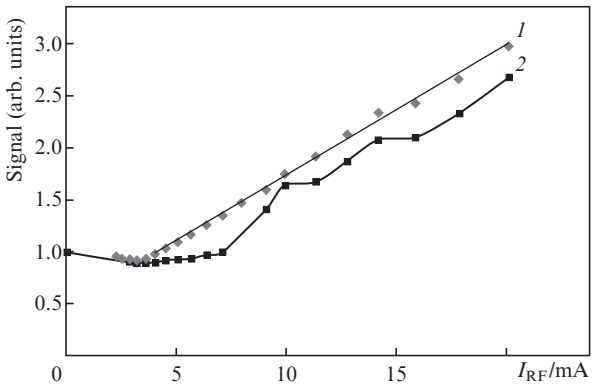

Figure 5. Dependences of (*1*) the laser emission power and (*2*) the sum of spectral band amplitudes on the rf current amplitude.

that actually over the whole range of rf currents the sum of the spectral band envelope amplitudes is less than the measured laser power. We explain this by broadening of the spectral bands due to presence of several rf components.

From the viewpoint of reducing light shifts, interesting are the spectral band pairs with the amplitude ratio of ~1, which are separated by an interval close to the clock transition frequency. Figure 6 presents the dependence of the frequency interval between chosen pairs of spectral bands on

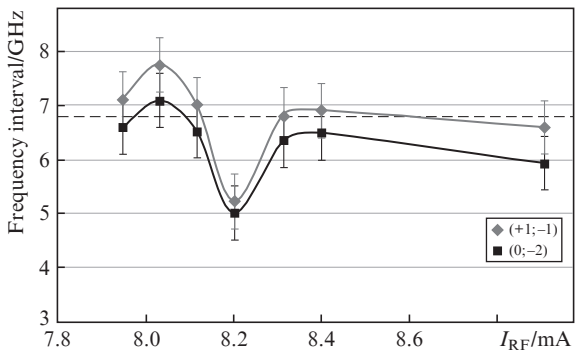

Figure 6. Dependence of the frequency interval between pairs of spectral bands (+1; –1) and (0; –2) on the rf current amplitude.

I_{RF} for the range of currents, in which the band amplitudes are close. The dashed line refers to the clock transition frequency (6.8 GHz). The measurement error for the spectral interval is related to the laser frequency drift relative to FPI transmission peaks. One can see that at certain values of frequency and rf current, the interval between the corresponding pairs equals the clock transition frequency. The nonlinear dependence of the interval between the bands of laser emission spectrum on the rf current, seemingly, refers to the dependence of Bessel function components on modulation index ε and to an influence of amplitude modulation. Hence, the maintenance of frequency difference for spectrum envelopes near the clock transition frequency requires certain accuracy while controlling the RF current.

5. Conclusions

Generation regimes are obtained for a diode laser pumped by rf-modulated current with the emission spectrum, in which the bands are separated by intervals mainly determined by the laser cavity length. Positions of side bands of laser emission in this case match the frequencies of optical transitions. The situation has been experimentally realised when the interval between spectral components was equal to the clock transition frequency and the ratio of their intensities was close to 1. This will reduce light shifts and, correspondingly, increase stability of the frequency standard.

Acknowledgements. The work was supported by the Ministry of Science and Higher Education of the Russian Federation in the framework of a base part of the State Task (Grant No. 3.6835.2017/8.9) and by the Russian Foundation for Basic Research (Grant No. 18-02-00316).

References

1. Arimondo E., Orriols G. *Lettere Al Nuovo Cimento*, **17**, 333 (1976).
2. Alzetta G., Gozzini A., Moi M., Orriols G. *Il Nuovo Cimento*, **36**, 5 (1976).
3. Vanier J. *Appl. Phys. B*, **81**, 421 (2005).
4. Bell W.E., Bloom A.L. *Phys. Rev. Lett.*, **6**, 280 (1961).
5. Vanier J., Levine M., Kendig S., Janssen D., Everson C., Delaney M. *Proc. IEEE Int. Ultrasonics, Ferroelectrics, Frequency Control Joint 50th Anniversary Conf.* (New York: IEEE, 2004) p. 92.
6. Khripunov S.A., Radnatarov D.A., Kobtcev S.M., Yudin V.I., Taichenachev A.V., Basalaev M.Yu., Balabas M.V., Andryushkov V.A., Popkov I.D. *Quantum Electron.*, **46**, 668 (2016) [*Kvantovaya Elektron.*, **46**, 668 (2016)].
7. Isakova A.A., Savinov K.N., Golovin N.N., Altynbekov N.Zh., Vishnyakov V.L., Dmitriev A.K. *Quantum Electron.*, **47**, 610 (2017) [*Kvantovaya Elektron.*, **47**, 610 (2017)].
8. Cyr N., Têtu M., Breton M. *IEEE Trans. Instrum. Meas.*, **42**, 640 (1993).
9. Stähler M., Wynands R., Knappe S., Kitching J., Hollberg L., Taichenachev A., Yudin V. *Opt. Lett.*, **27**, 1472 (2002).
10. Baklanov E.V., Dmitriev A.K. *Laser Phys.*, **20**, 52 (2010).
11. Bagayev S.N., Zakhar'yash V.F., Kashirskii A.V., Klement'ev V.M., Kuznetsov S.A., Pivtsov V.S. *Quantum Electron.*, **34**, 623 (2004) [*Kvantovaya Elektron.*, **34**, 623 (2004)].